# Letters

## Spread Spectrum Technique to Reduce EMI Emission for an *LLC* Resonant Converter Using a Hybrid Modulation Method

Hwa-Pyeong Park, *Member, IEEE*, Mina Kim, *Student Member, IEEE*, and Jee-Hoon Jung, *Senior Member, IEEE*

***Abstract*—A spread spectrum technique has been introduced to mitigate electromagnetic interference (EMI) in power converters. However, this technique is difficult to apply to resonant converters that use a pulse frequency modulation (PFM), because the spread spectrum can induce large output voltage fluctuations by PFM's switching frequency variations. In this letter, a hybrid control method using the PFM and phase shift modulation is proposed to obtain tight output voltage regulation under the spread spectrum operation of an *LLC* resonant converter. The performance of the proposed hybrid control method is experimentally verified using a 500 W prototype *LLC* resonant converter.**

***Index Terms*—Electromagnetic interference (EMI), *LLC* resonant converter, output voltage regulation, spread spectrum.**

### I. Introduction

ELECTROMAGNETIC interference (EMI) reduction has been a significant issue for implementing switch mode power supplies, since they should satisfy EMI standards [1]. Several EMI reduction methods have been proposed, such as passive and active EMI filters, soft-switching techniques, and spread spectrum techniques [2]–[7]. The spread spectrum has been introduced to mitigate the EMI [8]–[10] with several branches techniques such as sinusoidal, triangular, Hershey kiss, and random modulation. Fig. 1 shows the EMI reduction using the spread spectrum technique. It has switching frequency variations within the range of $f_c - \Delta f < f_c < f_c - \Delta f$, where $f_c$ is the carrier frequency and $\Delta f$ is the frequency deviation of the spread spectrum. The frequency modulation of the carrier frequency due to the spread spectrum is expressed as follows [10]:

$$s(t) = A_o \cos\left(2\pi f_c t + 2\pi\Delta f \int_{-\infty}^{t} \xi(\tau)\, d\tau\right) \qquad (1)$$

where $A_o$ is the amplitude of the signal, $-1 \le \zeta \le 1$ is the driving signal, which expresses the frequency variation for the spread spectrum. The power of $s(t)$ is equal to ${A_o}^2/2$, which can be scattered using the spread spectrum technique.

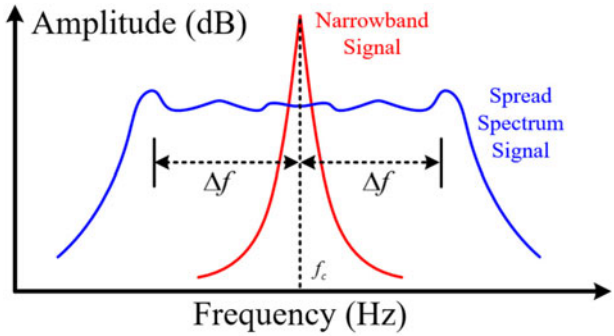


Fig. 1. Comparison between narrowband interfering signal and spread spectrum signal.

The spread spectrum technique has been widely applied to the power converters, such as buck and flyback converters, to suppress the EMI noise. The conventional converter topologies have very small input–output voltage gain changes according to the switching frequency variation. However, it generates the inductor current change, which induces the output voltage ripple. Therefore, the *L*–*C* output filter design according to the modulation frequency of the spread spectrum technique is significant to reduce the output voltage ripple [11].

The *LLC* resonant converter has been widely used in industry and consumer applications, such as home appliances, battery chargers, and data center server systems, since it has a higher power conversion efficiency with soft switching capability, and simple and cost-effective structure [12]–[15]. However, a pulse frequency modulation (PFM) can make the *LLC* resonant converter vulnerable to the EMI emission, because it changes the peak EMI frequency according to load variations. The spread spectrum technique can reduce the EMI emission of the *LLC* resonant converter. However, it has large output voltage fluctuation by the spread spectrum technique, because it induces the input–output voltage gain change by the switching frequency variation. In [16], the series resonant converter using the spread spectrum technique was proposed for an induction heating application. However, this application requires only input power regulation, which does not regulate the output voltage of the converter.

In this letter, the *LLC* resonant converter using the spread spectrum technique is proposed to reduce the EMI noise

Manuscript received June 29, 2017; revised August 2, 2017; accepted October 12, 2017. Date of publication October 25, 2017; date of current version February 1, 2018. This work was supported by the National Research Foundation of Korea under Grant NRF-2016R1A2B4011934. *(Corresponding author: Jee-Hoon Jung.)*

The authors are with the School of Electrical and Computer Engineering, Ulsan National Institute of Science and Technology, Ulsan 44919, South Korea (e-mail: darkrla6@unist.ac.kr; kmaop44@unist.ac.kr; jung.jeehoon@gmail.com).

Color versions of one or more of the figures in this letter are available online at http://ieeexplore.ieee.org.

Digital Object Identifier 10.1109/TPEL.2017.2766284

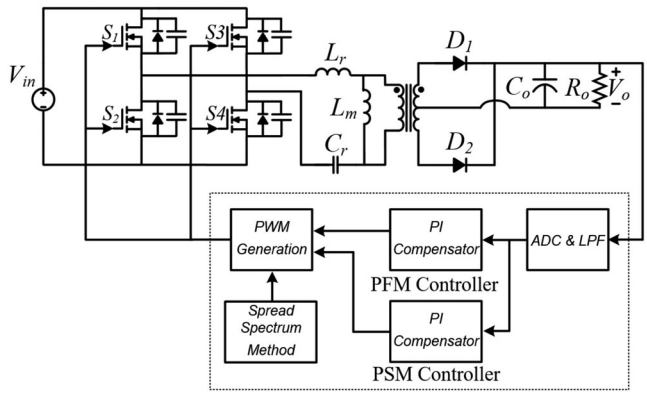


Fig. 2. Scheme of an *LLC* resonant converter for a spread spectrum technique.

emission. In addition, a hybrid control method using the PFM and phase shift modulation (PSM) is proposed to regulate the output voltage affected by the switching frequency variation of the spread spectrum technique. The triangular modulation is used as the spread spectrum technique. The PFM determines the carrier frequency of the spread spectrum according to the load variations. The instantaneous switching frequency is determined by the triangular modulation, but it can induce large output voltage fluctuation. The PSM is applied to compensate the output voltage fluctuation according to the switching frequency vibration caused by the spread spectrum. The output voltage variation by the switching frequency variation of the spread spectrum technique is analyzed with the output filter and the input–output voltage gain. The operational principle of the proposed control method is introduced to show the design methodology of the proposed control algorithm for suppressing the output voltage fluctuation as well as for reducing the EMI noise. The output voltage regulation and the EMI reduction performance using the spread spectrum are verified using a 500 W prototype *LLC* resonant converter and a digital controller (TMS320F28335 TI).

## II. Spread Spectrum Technique

### A. Control Algorithm for EMI Reduction

Fig. 2 shows the circuit diagram of the proposed *LLC* resonant converter, which has a full bridge structure to implement the PSM. It has the PFM and PSM controller to regulate the output voltage under the spread spectrum. After the PFM and PSM controller, the spread spectrum generator implements the triangular frequency modulation. The conventional PFM controller changes the switching frequency to compensate the output voltage variation according to the load variation. However, it is equal to the carrier frequency variation of the spread spectrum technique. The switching frequency variation mixed by the PFM and the spread spectrum cannot achieve the designed EM noise reduction as well as the output voltage regulation. In this letter, a hybrid control method is proposed, which has two operational modes to achieve the EM noise reduction and the output voltage regulation at the same time. First mode is the steady-state operation, and the second mode is the transient operation.

Fig. 3(a) shows the output voltage error variation in the proposed control algorithm. The proposed control algorithm has the borderline to the output voltage error to determine the

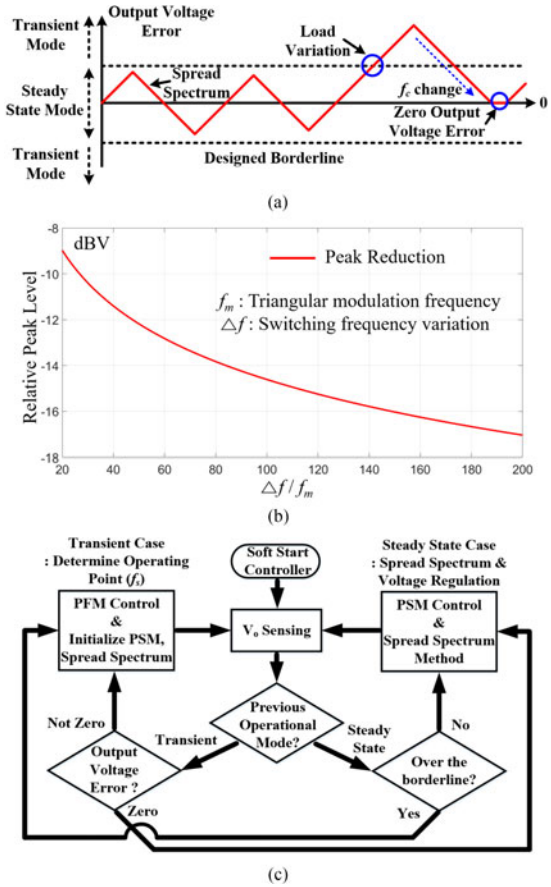


Fig. 3. Proposed control algorithm: (a) output voltage error variation; (b) peak conducted EMI level according to $\delta f/f_m$ ratio; and (c) control sequences.

operational modes. In the steady-state mode, the triangular frequency modulation changes the switching frequency to implement the spread spectrum. The PSM only operates to regulate the output voltage of the *LLC* resonant converter. The PFM does not operate in this mode because of the triangular frequency modulation for the spread spectrum. Therefore, the controller regulates the output voltage using the PSM under the spread spectrum with the triangular frequency modulation. The reduction of EMI peak using the spread spectrum was introduced in [9]. The large switching frequency variation ($\Delta f$) and the low triangular modulation frequency ($f_m$) can reduce the peak EMI value. Fig. 3(b) shows the relative peak level reduction according to the $\Delta f/f_m$ ratio. In this letter, the designed EMI peak reduction is 14 dB$\mu$V less than no spread spectrum case.

If the output voltage error is over the borderline, the controller operates in the transient mode. In this mode, the PFM rearranges the carrier frequency to regulate the output voltage, because the PSM has a limited output voltage regulation range. In addition, small phase shift induces small circulating power and rms current. The PSM and the triangular frequency modulation do not operate in the transient mode but initialize these values. If the output voltage error is converged to zero, the controller operates in the steady-state mode. Fig. 3(c) shows the block diagram of the proposed control algorithm. It also shows two operational conditions to implement the spread spectrum technique and the output voltage regulation.

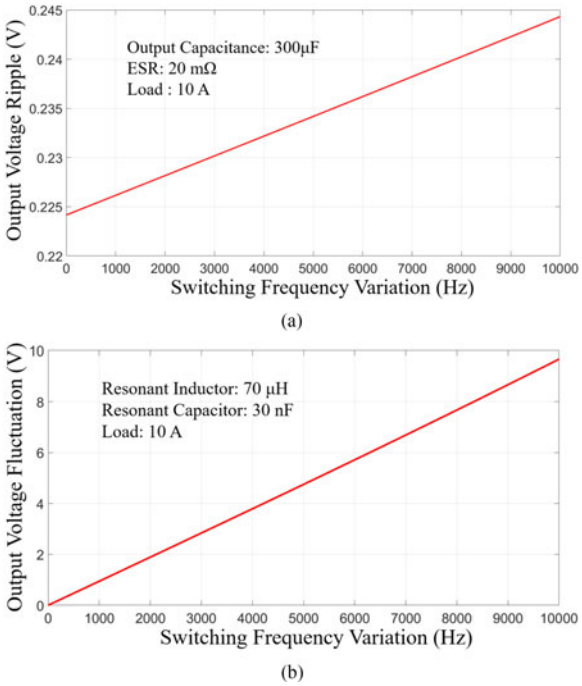


Fig. 4. Comparison of output voltage variation according to switching frequency variation: (a) considering output capacitance and (b) considering the input–output voltage gain change.

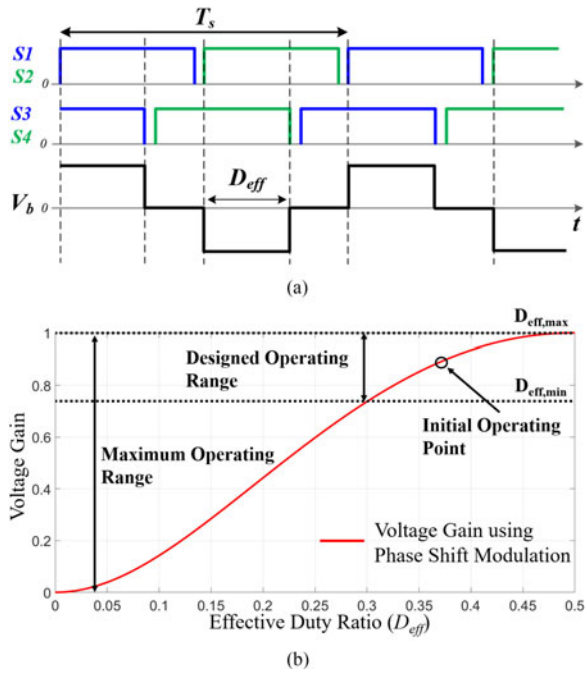


Fig. 5. PSM control method: (a) operational waveform of PSM and (b) voltage gain of PSM.

### B. Output Voltage Regulation

The spread spectrum technique for the conventional PWM converters generates the output voltage ripple, because switching frequency variation induces the inductor current variation. The slow modulation frequency of the spread spectrum technique can reduce the EMI noise, effectively, as shown in Fig. 3(b). However, the low modulation frequency requires the large output capacitance to suppress the output voltage ripple with low cut-off frequency. The conventional buck converters have to consider the cut-off frequency of the *L–C* output filter for decreasing the output voltage ripple. In [11], the effect of a spread spectrum method on the output voltage ripple was discussed. In the *LLC* resonant converter, output voltage ripple with the output filter can be derived as follows [17]:

$$\Delta V\left(f_s\right) = \mathrm{ESR} \times \left(\frac{\pi}{2} - 1\right) \times I_o + \frac{\Delta Q}{C_o} \tag{2}$$

where ESR is the effective series resistance of the output capacitor, $I_o$ is the load current, and $\Delta Q = 0.363 I_o T_s$. Considering the spread spectrum, the switching frequency variation can be expressed as $f_s + \Delta f_{\max}$ and $f_s - \Delta f_{\max}$. $\Delta f_{\max}$ is the maximum switching frequency variation. From (2), the output voltage ripple at the output filter can be derived as follows:

$$\Delta V_{\text{filter}} = \Delta V\left(f_s - \Delta f_{\max}\right) - \Delta V\left(f_s + \Delta f_{\max}\right). \tag{3}$$

It shows that the large output capacitor is needed to suppress the output voltage ripple against the switching frequency variation.

Compared with the conventional PWM converters, the *LLC* resonant converter has serious output voltage fluctuation caused by the input–output voltage gain change according to the switching frequency variation. Using the spread spectrum technique, the maximum output voltage fluctuation of the *LLC* resonant converter can be derived as follows:

$$\Delta V_{o,\max} = \frac{G\left(f_s + \Delta f_{\max}\right) \cdot V_{\text{in}} - G\left(f_s - \Delta f_{\max}\right) \cdot V_{\text{in}}}{n} \tag{4}$$

where $G(f)$ is the converters input-to-output voltage gain, $V_{\text{in}}$ is the input voltage, and $n$ is the transformers turn ratio. It shows that the large switching frequency vibration from the spread spectrum can induce serious output voltage fluctuation without any compensating techniques. The output voltage fluctuation according to the voltage gain change is determined with the resonant tank design and switching frequency variation. The theoretical output voltage ripple by the spread spectrum technique is shown in Fig. 4(a) and (b). It shows that the output voltage ripple by the output capacitor is negligible than the output voltage fluctuation from the input–output voltage variation. Therefore, the solution to suppress the output voltage fluctuation is required for the resonant converters.

The PSM is adopted to compensate the output voltage fluctuation caused by the spread spectrum in the steady-state operation. The PSMs voltage gain can be derived as shown in (5) at the bottom of the page [18], where $d_{\text{eff}}$ is the amount of the phase shift using the PSM, $f_n$ is the normalized frequency ($f_s/f_{s,n}$), $f_{s,n}$ is the reference switching frequency, $k$ is the magnetizing

$$G(d_{\text{eff}}) = \frac{1 - \cos\left(2\pi d_{\text{eff}}/f_n\right)}{1 + \frac{4Q}{\pi f_n} - \frac{\pi^2 d_{\text{eff}}}{k f_n^2}\left(\frac{1}{2} - d_{\text{eff}}\right) + \cos\left(\frac{2\pi d_{\text{eff}}}{f_n}\right)\left[\frac{4Q}{\pi f_n} + \frac{\pi^2 d_{\text{eff}}}{k f_n^2}\left(\frac{1}{2} - d_{\text{eff}}\right) - 1\right] + \frac{\pi d_{\text{eff}}}{k f_n}\sin\left(\frac{2\pi d_{\text{eff}}}{f_n}\right)} \tag{5}$$

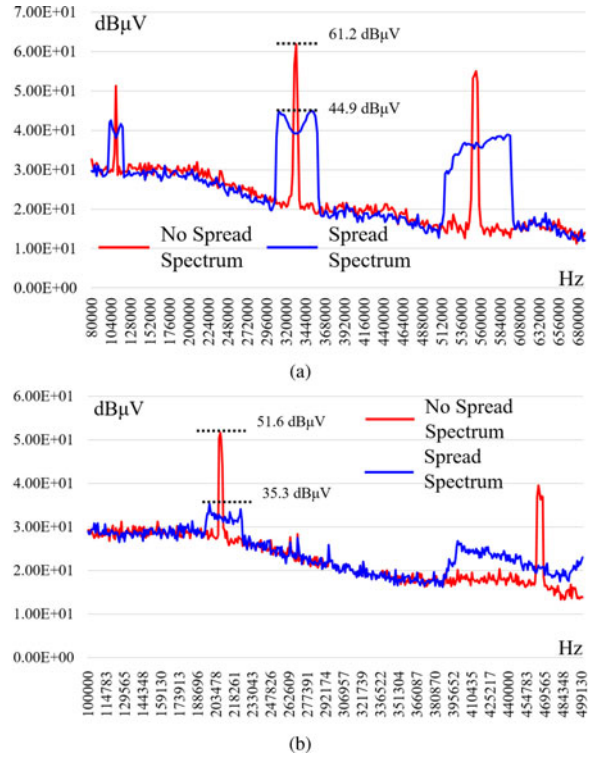


Fig. 6. Reduction of EMI noise: (a) common mode noise and (b) and differential mode noise.

TABLE I
DESIGN SPECIFICATIONS OF 500 W PROTOTYPE CONVERTER

| Parameter | Experimental value |
|---|---|
| $V_{\text{in}}$ | 400 V |
| Load condition | 50 V, 10 A |
| Resonant capacitor | 30 nF |
| Resonant inductance | 70 $\mu$H |
| Magnetizing inductance | 290 $\mu$H |
| $\Delta f$ | 7 kHz |
| $f_m$ | 80 Hz |

TABLE II
PERFORMANCE COMPARISON

| Measured results | No spread spectrum | Spread spectrum without compensation |
|---|---|---|
| Peak CM noise | 61.2 dB$\mu$V | 46.2 dB$\mu$V |
| Peak DM noise | 51.6 dB$\mu$V | 36.1 dB$\mu$V |
| Output voltage ripple | 2.544 $V_{pp}$ | 6.616 $V_{pp}$ |
| Measured results | Spread spectrum with compensation | |
| Peak CM noise | 44.9 dB$\mu$V | |
| Peak DM noise | 35.3 dB$\mu$V | |
| Output voltage ripple | 3.857 $V_{pp}$ | |

and the resonant inductance ratio ($L_m/L_r$), and $Q$ is the quality factor. Fig. 5(a) and (b) shows the operational waveforms and the voltage gain of the PSM, respectively. In Fig. 5(b), the PSM can achieve only step-down in the output voltage. The initial operating point of the PSM is important to compensate the output voltage error according to the spread spectrum, because it requires both the step-up and step-down capabilities in the output voltage. The required voltage gain using the PSM can be

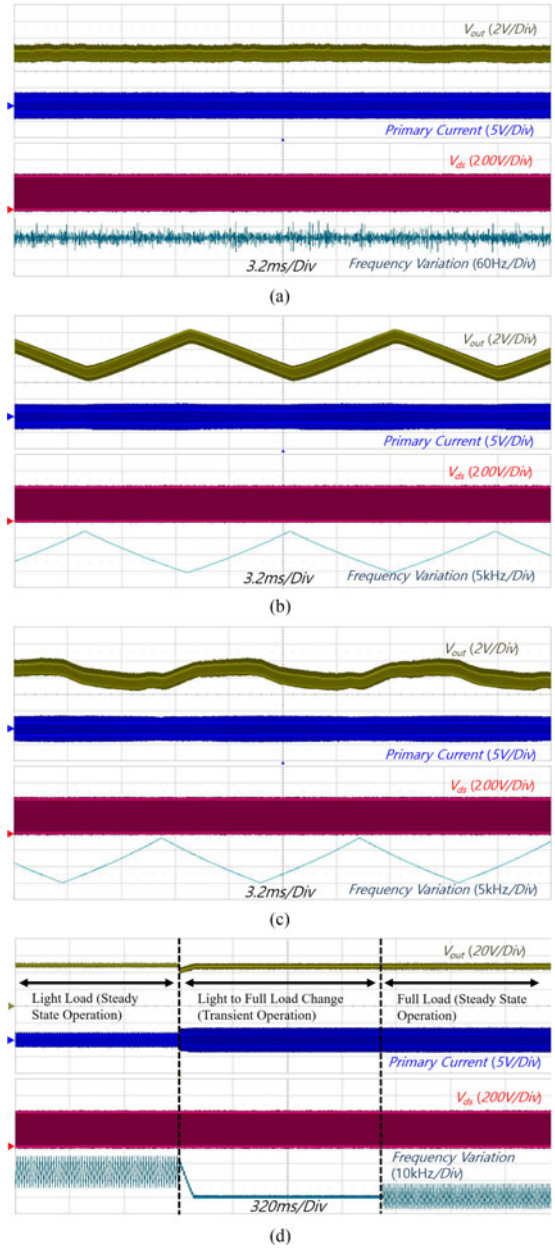


Fig. 7. Operational waveforms: (a) no spread spectrum; (b) spread spectrum without compensation; (c) spread spectrum with compensation; and (d) mode transition.

derived as follows:

$$G_{\text{re}} = G\left(f_c + \Delta f_{\max}\right) \cdot G\left(d_{\text{eff,max}}\right) = G\left(f_c - \Delta f_{\max}\right) \cdot G\left(d_{\text{eff,min}}\right) \quad (6)$$

where $d_{\text{eff,min}}$ and $d_{\text{eff,max}}$ are the designed minimum and maximum effective duty ratio, respectively, and $G_{\text{re}}$ is the required voltage gain. The initial operating point can be derived as $G(d_{\text{eff,ini}}) = [G(d_{\text{eff,max}}) + G(d_{\text{eff,min}})]/2$. However, the voltage gain compensation using the PSM has a limited range. Fig. 5(b) shows the available minimum and maximum voltage gain range using the PSM. Under the maximum compensation condition, the initial operating point ($d_{\text{eff,ini}}$) is half of the PSM voltage gain, which can be expressed as $G(d_{\text{eff,ini}}) = G(d_{\text{eff,max}})/2$. Therefore, the minimum and maximum voltage gain variation by the spread

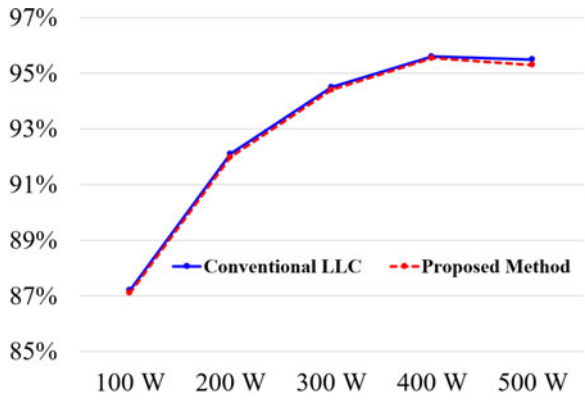


Fig. 8. Comparison of power conversion efficiency between the proposed hybrid modulation technique and the conventional PFM modulation according to load variations.

spectrum can be expressed as $G(f_c + \Delta f_{\max}) = G(f_c)/2$ and $G(f_c - \Delta f_{\max}) = 2G(f_c)$, respectively. The available maximum switching frequency range is changed by the resonant tank and the load condition, because the voltage gain curve shape and sharpness of the *LLC* resonant converter are affected by the quality factor, the magnetizing inductance, and load condition. Under the light load condition, the *LLC* resonant converter has high voltage gain sharpness, which can be design reference to determine the maximum switching frequency variation range.

## III. Experimental Results

Fig. 6(a) and (b) shows the peak common mode (CM) and differential mode (DM) noises, respectively. The spread spectrum technique using the triangular modulation reduces the EM noise effectively. The specification of the power converter and the spread spectrum technique used in the experiment is described in Table I. Fig. 7 shows the comparison of the output voltage regulation performance. If the PSM is not used to compensate the output voltage ripple according to the spread spectrum, the *LLC* resonant converter has 2.6 times higher output voltage ripple than the no spread spectrum case, as shown in Fig. 7(b). However, the PSM compensation has 0.58 times smaller output voltage ripple than the no compensation case, as shown in Fig. 7(c), which is 1.5 times higher output voltage ripple than the no spread spectrum case. Table II shows the comparison of the output voltage fluctuation and the EM noise. The power supplies for the home appliances, such as TV and computer, have low dropout regulators (LDOs) or small-sized converter after the main power supply. Therefore, in those applications, the output voltage variation around ten percent can be acceptable for those systems. In addition, dc motor applications such as printers can operate under ten percent output voltage fluctuation. Fig. 7(d) shows mode change cases between the steady-state and the transient modes. In the step-load variation, it shows the output voltage regulation using the proposed modulation method. Fig. 8 shows the comparison of the power conversion efficiency between the proposed hybrid modulation technique and the conventional PFM method. There is no difference between two efficiency curves according to the load variation.

## IV. Conclusion

In this letter, the PFM and PSM hybrid control algorithm is proposed to implement the spread spectrum technique and to achieve tight output voltage regulation for the *LLC* resonant converter. The operational principles of the proposed control algorithm are analyzed to reduce the EM noise and the output voltage fluctuation. The experimental results show the EM noise reduction ($-12.9$ dB$\mu$V on DM and $-16.1$ dB$\mu$V on CM). In addition, the proposed control algorithm shows 0.58 times smaller output voltage fluctuation than the case of using the spread spectrum without compensation.

## References

[1] FCC, "Code of federal regulations 47 (47CFR), Part 15, Subpart B: Unintentional radiators." [Online]. Available: http://www.ecfr.gov/. Accessed on: Jun. 27, 2017.

[2] K. Raggl, T. Nussbaumer, and J. W. Kolar, "Guideline for a simplified differential-mode EMI filter design," *IEEE Trans. Ind. Electron.*, vol. 57, no. 3, pp. 1031–1040, Mar. 2010.

[3] M. C. D. Piazza, A. Ragusa, and G. Vitale, "Power-loss evaluation in CM active EMI filters for bearing current suppression," *IEEE Trans. Ind. Electron.*, vol. 58, no. 11, pp. 5142–5153, Nov. 2011.

[4] S. W. D. Fu, P. Kong, F. C. Lee, and D. Huang, "Novel techniques to suppress the common-mode EMI noise caused by transformer parasitic capacitances in dc-dc converters," *IEEE Trans. Ind. Electron.*, vol. 60, no. 11, pp. 4968–4977, Nov. 2013.

[5] D. Gonzalez *et al.* "Conducted EMI reduction in power converters by means of periodic switching frequency modulation," *IEEE Trans. Power Electron.*, vol. 22, no. 6, pp. 2271–2281, Nov. 2007.

[6] K. K. Tse, H. S. H. Chung, S. Y. Huo, and H. C. So, "Analysis and spectral characteristics of a spread-spectrum technique for conducted EMI suppression," *IEEE Trans. Power Electron.*, vol. 15, no. 2, pp. 399–410, Mar. 2000.

[7] S. Kapat, "Reconfigurable periodic bifrequency DPWM with custom harmonic reduction in dcdc converters," *IEEE Trans. Power Electron.*, vol. 31, no. 4, pp. 3380–3388, Apr. 2016.

[8] O. Trescases, A. P. G. Wei, and W. T. Ng, "An EMI reduction technique for digitally controlled SMPS," *IEEE Trans. Power Electron.*, vol. 22, no. 4, pp. 1560–1565, Jul. 2007.

[9] F. Pareschi, G. Setti, R. Rovatti, and G. Frattini, "Practical optimization of EMI reduction in spread spectrum clock generators with application to switching dc/dc converters," *IEEE Trans. Power Electron.*, vol. 29, no. 9, pp. 4646–4657, Sep. 2014.

[10] F. Pareschi, R. Rovatti, and G. Setti, "EMI reduction via spread spectrum in dc/dc converters: State of the art, optimization, and tradeoffs," *IEEE Acesss*, vol. 3, pp. 2857–2874, 2015.

[11] J. Jankovskis, D. Stepins, and N. Ponomarenko, "Effects of spread spectrum on output filter of buck converter," *Elektronika ir Elektrotechnika*, vol. 19, no. 5, pp. 45–48, May 2013.

[12] R. Beiranvand, B. Rashidian, M. R. Zolghadri, and S. M. H. Alavi, "Using LLC resonant converter for designing wide-range voltage source," *IEEE Trans. Ind. Electron.*, vol. 58, no. 5, pp. 1746–1756, May 2011.

[13] H. P. Park and J. H. Jung, "PWM and PFM hybrid control method for LLC resonant converters in high switching frequency operation," *IEEE Trans. Ind. Electron.*, vol. 64, no. 1, pp. 253–263, Jan. 2017.

[14] B. Gu, C. Y. Lin, B. Chen, J. Dominic, and J. S. Lai, "Zero-voltage-switching PWM resonant full-bridge converter with minimized circulating losses and minimal voltage stresses of bridge rectifiers for electric vehicle battery chargers," *IEEE Trans. Power Electron.*, vol. 28, no. 10, pp. 4657–4667, Oct. 2013.

[15] Z. Fang, T. Cai, S. Duan, and C. Chen, "Optimal design methodology for LLC resonant converter in battery charging applications based on time-weighted average efficiency," *IEEE Trans. Power Electron.*, vol. 30, no. 10, pp. 5469–5483, Oct. 2015.

[16] L. A. Barragan, D. Navarro, J. Acero, I. Urriza, and J. M. Burdio, "FPGA implementation of a switching frequency modulation circuit for EMI reduction in resonant inverters for induction heating appliances," *IEEE Trans. Ind. Electron.*, vol. 55, no. 1, pp. 11–20, Jan. 2008.

[17] H.-P. Park, Y. Rye, K. J. Han, and J.-H. Jung, "Design considerations of resonant network and transformer magnetics for high frequency LLC resonant converter," *J. Electr. Eng. Technol.*, vol. 11, no. 2, pp. 383–392, Nov. 2016.

[18] J. H. Kim, C. E. Kim, J. K. Kim, J. B. Lee, and G. W. Moon, "Analysis on load-adaptive phase-shift control for high efficiency full-bridge LLC resonant converter under light-load conditions," *IEEE Trans. Power Electron.*, vol. 31, no. 7, pp. 4942–4955, Jul. 2016.